Assessing the Water-Stress Baselines by Thermal Imaging for Irrigation Management in Almond Plantations under Water Scarcity Conditions

Saray Gutiérrez-Gordillo [1,*] , **Iván Francisco García-Tejero** [1] , **Víctor Hugo Durán Zuazo** [2] , **Amelia García Escalera** [1], **Fernando Ferrera Gil** [1], **José Juan Amores-Agüera** [1], **Belén Cárceles Rodríguez** [2] and **Virginia Hernández-Santana** [3]

[1] Instituto Andaluz de Investigación y Formación Agraria y Pesquera (IFAPA), Centro "Las Torres-Tomejil", Carretera Sevilla-Cazalla Km 12.2, 41200 Alcalá del Río (Sevilla), Spain; ivanf.garcia@juntadeandalucia.es (I.F.G.-T.); ameliagaes7@gmail.com (A.G.E.); fernandoferreragil@icloud.com (F.F.G.); josej.amores@juntadeandalucia.es (J.J.A.-A.)

[2] Instituto Andaluz de Investigación y Formación Agraria y Pesquera (IFAPA), Centro "Camino de Purchil", Camino de Purchil s/n, 18004 Granada, Spain; victorh.duran@juntadeandalucia.es (V.H.D.Z.); belen.carceles@juntadeandalucia.es (B.C.R.)

[3] Instituto de Recursos Naturales y Agrobiología de Sevilla, Consejo Superior de Investigaciones Científicas, Avda. Reina Mercedes 10, 41012 Sevilla, Spain; virginiahsa@irnas.csic.es

*   Correspondence: saray.gutierrez@juntadeandalucia.es; Tel.: +34-671532852

check for updates

Abstract: This work examines the use of thermal imaging to determine the crop water status in young almond trees under sustained deficit irrigation strategies (SDIs). The research was carried out during two seasons (2018–2019) in three cultivars (*Prunus dulcis* Mill., cvs. Guara, Lauranne, and Marta) subjected to three irrigation treatments: a full irrigation treatment (FI) at 100% of irrigation requirements (IR), and two SDIs that received 75% and 65% of the IR, respectively. Crop water monitoring was done by measurements of canopy temperature, leaf water potential (Ψ_{leaf}), and stomatal conductance. Thermal readings were used to define the non-water-stress baselines (NWSB) and water-stress baselines (WSB) for each treatment and cultivar. According to our findings, Ψ_{leaf} was the most responsive parameter to reflect differences in almond water status. In addition, NWSB and WSB allowed the determination of the crop water-stress index (CWSI) and the increment of canopy temperature (IT_C) for each SDI treatment, obtaining threshold values of CWSI (0.12–0.15) and IT_C (~1 °C) that would ensure maximum water savings by minimizing the effects on yield. The findings highlight the importance of determining the different NWSB and WSB for different almond cultivars and its potential use for proper irrigation scheduling.

Keywords: thermography; irrigation scheduling; thermal indexes; crop water status

1. Introduction

Irrigation performs an essential role in agriculture. As such, the increase in total irrigated area, coupled with scarce water resources, has encouraged the implementation of irrigation strategies that optimize the water-use efficiency. Specifically, in areas such as southern Spain, this supply is crucial for the proper development of woody crops, when the maximum evapotranspiration rates coincide with the rainfall absence. Considering the current scenarios of climatic change and water scarcity, the adaptation and sustainable strategies to boost the proper water management in irrigated crops is vital [1]. Among them, deficit irrigation (DI) has been implemented to enhance the yield, reducing the irrigation supplies and maximizing the crop productivity [2]. According to this, the implementation

of DI in many arid and semi-arid irrigated areas has been addressed, especially in representative Mediterranean woody species, namely olive [3], mango [4], walnut [5], citrus [6], or pistachio [7], among others.

Almond (*Prunus dulcis* Mill.) is considered as drought-tolerant crop, and for the case of Spain it has been traditionally cultivated in rainfed and marginal areas; although, recently, its presence in irrigated areas has progressively increased [8]. Because of the representativeness of this crop in arid and semi-arid regions, many authors have already studied its yield response to DI strategies, obtaining significant improvements in terms of water savings without substantial losses in almond yield [9–11]. In addition, different experiments have corroborated that the optimum period to apply moderate-to-severe water restrictions coincides with stage IV (kernel-filling period) [12,13], and hence, most of them have been developed introducing different water withholdings during this period.

Moreover, the success of applying a proper irrigation schedule based on DI strategies requires crop water monitoring by means of plant-based measurements, defining thresholds to maintain water restrictions during phenological development without compromising the final production [14]. Traditionally, this assessment has been done by punctual measurements of stem or leaf water potential (Ψ_{leaf}) or stomatal conductance (g_s), with high representation of the crop water status but a low convenience and practical usage [15], hampering the taking of decisions for irrigation scheduling [16]. Alternatively, canopy temperature (T_C) and the related thermal indexes have been recognized as proper indicators of crop water status [17,18], because of their relationship with crop transpiration rates [19]; hence, techniques that are less time-consuming, such as thermography, have been widely accepted [20–23]. Thus, when water restrictions are applied, the plant responds by closing the stomata (reducing g_s and transpiration), minimizing the water losses by the leaf and, therefore, increasing the leaf temperature.

Additionally, thermal imaging provides information of the whole canopy, and hence this technique offers the possibility of developing fast spatio-temporal measurements and water status monitoring on a whole-plant basis [24]. However, in accordance with Jones [25] and Jones and Vaughan [26], there are many climatic variables, such as radiation, atmospheric temperature, vapor pressure deficit (VPD), relative humidity, wind, or air convection, that may influence the leaf temperature; thus, not only the water status effects. Therefore, to avoid the effects of these environmental variables, thermal indexes to monitor crop water stress have been defined to normalize the absolute canopy temperature (Tc) readings, such as the crop water-stress index (CWSI), the thermal index to relative stomatal conductance (I_G), or the difference between the canopy and air temperature ($\Delta T_{canopy-air}$) [25,27]. In the case of CWSI or I_G, reference values for well-watered and non-transpiring T_C are required, which provide theorical lower and upper T_C values for the current environmental conditions. This fact substantially hampers the applicability of these indexes, which normally are obtained by means of artificial measurements of reference materials or leaves that have been previously exposed to modified conditions, which is rather complex and time-consuming [22,23]. To prevent these constraints, the difference between the air and canopy temperature ($\Delta T_{canopy-air}$) is widely used as a simpler thermal index, offering interesting results for crop-water monitoring and irrigation scheduling [28]. Even so, $\Delta T_{canopy-air}$ can substantially change because of other environmental conditions. In order to solve this situation, non-water-stress baselines (NWSB) and water-stress baselines (WSB) are defined. These linear functions relates the values of $\Delta T_{canopy-air}$ with the VPD registered during the T_C readings [22] for fully irrigated and DI strategies, respectively. Moreover, these WSBs can be defined for different levels of water restrictions, establishing a correspondence between a hypothetical WSB and the potential yield losses induced by the water stress imposed.

In addition, when these baselines are obtained under fully irrigated conditions, these can be used to determine the lower and upper limits for the CWSI estimation, as was suggested by Idso et al. [29], enabling the irrigation scheduling and taking decisions.

Furthermore, the NWSB permits to compute the increment of T_C (IT_C), which is the difference between the $\Delta T_{canopy-air}$ obtained for a hypothetical irrigation strategy and its corresponding NWSB

value, using the VPD of that particular day [14]. In this line, one step further towards to DI programming would be to obtain the most appropriate WSB, which would correspond to that obtained for the treatment, and ensure the maximum water saving and minimum yield loss. Moreover, this WSB would allow defining the threshold IT_C, providing the advisable value for the maximum deviation from the NWSB.

Taking these points into consideration, the objectives of this study were (i) to determine the NWSB for three studied almond cultivars during the kernel-filling period; (ii) to define the WSB for two different water-stress levels; and (iii) to establish a protocol to manage the irrigation scheduling by means of these functions and its relation with the yield.

2. Materials and Methods

2.1. Experimental Site

The experiment was conducted during the kernel-filling and postharvest period (June to September) in two consecutive years (2018 and 2019), in a commercial almond (*P. dulcis* Mill. cvs. Guara, Marta, and Lauranne) orchard, grafted onto GN15 rootstock, and located in the Guadalquivir river basin (SW Spain, 37°30′27.4″ N, 5°55′48.7″ W). Trees were planted in 2013, spaced 8 m × 6 m, and drip irrigated using two pipelines with emitters of 2.3 L × h^{-1}, spaced at 0.75 m intervals. Canopy volumes were very similar within each cultivar, without differences between irrigation treatments. Thus, for Marta, canopy volumes ranged between 64 and 65 m^3; Guara trees, between 65 and 66 m^3; and Lauranne, trees between 72 and 74 m^3.

The soil was a silty loam, a typical Fluvisol, more than 2 m deep, with organic matter <1.5%. Roots were located predominately in the first 50 cm of the soil, corresponding to the intended wetting depth. Soil water content values at field capacity (−0.33 MPa) and permanent wilting point (−1.5 MPa) were close to 0.40 and 0.15 m^3 × m^{-3}, respectively.

The climatic classification of the study area was attenuated meso-Mediterranean with a hot-summer Mediterranean climate (csa) in the Köppen climate classification [30], with an annual ET_0 rate of 1400 mm, an average temperature of 18 °C, and accumulated rainfall of 540 mm (average data corresponding to the last 15 years (2004–2019); obtained from the Andalusian Weather information Network).

2.2. Irrigation Treatments

Three irrigation treatments were designed as follows: (i) a fully irrigated treatment (FI), which received 100% of the irrigation requirements (IR) during the whole irrigation period; (ii) a sustained deficit irrigation (SDI_{75}) treatment, which received 75% of the IR; and (iii) a sustained deficit irrigation (SDI_{65}), which received 65% of the IR.

In both seasons, irrigation was applied from the middle of March to the end of October, and these doses were calculated according to the methodology proposed by Allen et al. [31] (Equations (1) and (2)); obtaining the values of reference evapotranspiration (ET_0) by using a weather station installed in the same experimental orchard (Davis Advance Pro2, Davis Instruments, Valencia, Spain).

$$ET_C = K_C \times K_r \times ET_0 \tag{1}$$

$$IR \text{ (mm)} = (ET_C - Rainfall) \tag{2}$$

where ET_C is the crop evapotranspiration; K_C is the single-crop coefficient; Kr is the crop reduction coefficient, which depends on the percentage of shaded area cast by the tree canopy; ET_0 is the reference evapotranspiration; and IR is the irrigation requirements.

The local monthly K_C and K_r used during the experimental period are shown in Table 1, as was determined by García-Tejero [32]. Additionally, the IR was reduced for SDI_{75} and SDI_{65} by multiplying it by 0.75 and 0.65, respectively.

Table 1. Local crop reduction and crop coefficient values used in the experiment.

Coefficients	March	April	May	June	July	August	September	October
K_C	0.4	0.6	0.9	1.1	1.2	1.1	0.8	0.7
K_r	0.4	0.7	0.8	0.9	0.9	0.8	0.8	0.7

2.3. Plant Measurements

During the kernel-filling period (162–225 days of the year (DOY) in 2018; and 162–217 DOY in 2019), crop water monitoring was done throughout the measurements of the leaf water potential (Ψ_{leaf}), stomatal conductance, water vapor (g_s), and canopy temperature (T_C); all these readings were taken between 12:00 and 13:30 GTM, and with a periodicity of 7–10 days.

The g_s was measured using a porometer SC-1 (Decagon Devices, INC, WA, USA) in two leaves per tree (monitoring 8 trees per irrigation treatment) fully developed, and completely exposed to the sun, with the aim of monitoring the maximum values of g_s and detecting the most detectable differences among the irrigation treatments. The selected leaves were at 1.5 m of height, approximately, and were SE facing. On the other hand, the Ψ_{leaf} was measured using a pressure chamber (Soil Moisture Equipment Corp., Sta. Barbara, CA, USA), monitoring two leaves per tree, located on the north side of the tree and being totally mature, fresh and shaded, with the aim of minimizing the measurements variability. Selected leaves were at 1.5 m of height, approximately, and NW facing.

Considering the results obtained by García-Tejero et al. [33], who reported that the best moment for assessing the T_C was between 11:30 and 14:30, and in the sunny side of canopy, thermal images were taken following this procedure: using a ThermaCam (Flir SC660, Flir System, USA, 7–13 μm, 640 × 480 pixels) and an emissivity (ε) of 0.96 (Figure 1). Readings were developed at the sunny side of the canopy, placing the camera at a 4 m distance from the monitored tree, approximately. Afterwards, images were analyzed using the Flir Research Pro Software (Flir System, USA), which allows to select different zones of the images (in our case; 4 different sunny areas per image were selected); each pixel corresponding to an effective temperature value [19].

Once the images were obtained, T_C was calculated for each treatment, cultivar, and monitoring day, and after this, the thermal index $\Delta T_{canopy\text{-}air}$ was calculated. Taking into consideration the $\Delta T_{canopy\text{-}air}$ values and the VPD registered during the data acquisition, the NWSB and WSB were defined according to Equation (3); these functions corresponding to trees that were subjected to different irrigation doses, and allow to estimate the optimum values of $\Delta T_{canopy\text{-}air}$ for each treatment depending on the VPD values [29].

$$\Delta T_{canopy-air} = b + a \times VPD \tag{3}$$

where b and a are the intercept point and slope of the linear function.

Additionally, taking as reference the NWSB obtained for each cultivar, the CWSI along the monitoring period for each DI treatment was estimated, according to Equations (4) and (5):

$$CWSI = \frac{\Delta T_{canopy-air} - \Delta T_{wet}}{\Delta T_{dry} - \Delta T_{wet}} \tag{4}$$

where $\Delta T_{canopy\text{-}air}$ corresponds to the canopy readings obtained in each treatment and cultivar; ΔT_{wet} is the lower limit calculated from the NWSB equation in each cultivar; and ΔT_{dry} is the upper limit obtained according to the methodology proposed by Idso et al. (1981).

$$\Delta T_{dry} = b + a[e_s(T_{air}) - e_s(T_{air} + b)] \tag{5}$$

where a and b are the slope and the interception point for the NWSB; $e_s (T_{air})$ is the saturated vapor pressure at air temperature; and $e_s (T_{air} + b)$ is the saturated vapor pressure at the sum of the air temperature and interception point.
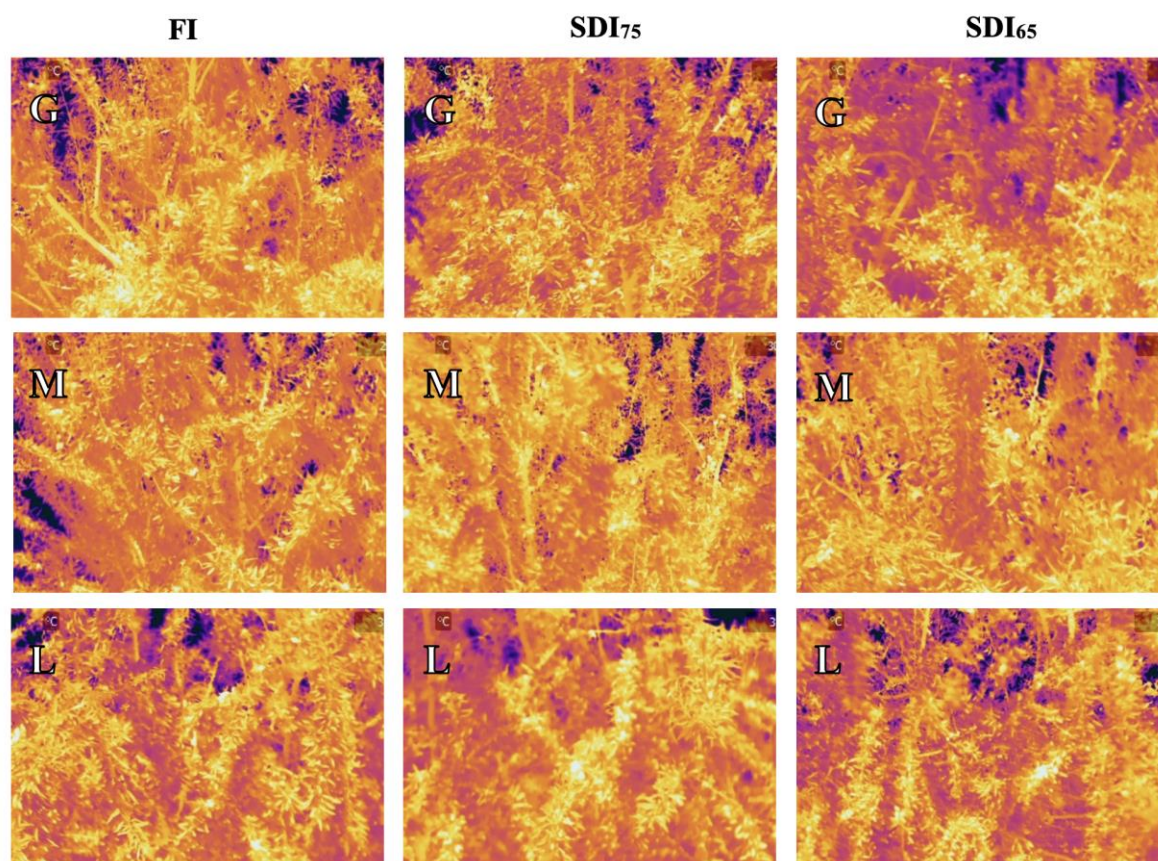
Figure 1. Thermal images at the sunny side of the studied almond canopies. FI, fully irrigated treatment; SDI$_{75}$, sustained deficit irrigation treatment at 75% of the irrigation requirements; SDI$_{65}$, sustained deficit irrigation treatment at 65% of the irrigation requirements; G, Guara; M, Marta; L, Lauranne.

2.4. Experimental Design and Statistical Analysis

The experimental design was of randomized blocks, with four replications per irrigation treatment and cultivar. Each replication had 12 trees (3 rows and 4 trees per row); the two central trees for each replication were monitored. Thus, eight trees per irrigation strategy treatment were used. Statistical analysis was done by using the Sigma Plot statistical software (version 12.5, Systat Software, Inc., San Jose, CA, USA). For each measurement day, an exploratory and descriptive analysis of the data (T$_C$, Ψ_{leaf}, and g$_s$) was developed, applying a Levene's test to check the variance homogeneity of the variables studied. Significant differences among irrigation treatments ($p \leq 0.05$) were identified by applying a one-way ANOVA, and a Tukey's test to identify the significant differences. Additionally, there were defined the NWSB and WSB for each irrigation treatment and cultivar, analysing the differences by applying an ANCOVA to evaluate the differences in the interception points and slopes, and obtaining the threshold values of the CWSI and IT$_C$ for each cultivar that ensure minimum yield loss and the highest water saving. For this, at the end of each season, the effects on kernel yield in relation to irrigation treatments were analyzed by applying a one-way ANOVA, and a Tukey's test to identify the significant differences.

3. Results

3.1. Climate Condition and Irrigation Water Amount Applied

Table 2 shows the climatic conditions during the two studied seasons. During the irrigation period (from April to October), the cumulative rainfall was 326 and 85 mm for 2018 and 2019, respectively. In relation to ET_C, similar values for 2018 and 2019 (~880 and 840 mm respectively) were registered. This fact, together with the high differences in terms of rainfall, promoted that the irrigation doses applied in the studied treatments were much greater in the second experimental season. In this sense, FI, SDI_{75}, and SDI_{65} received 4974, 3713, and 3342 $m^3 \cdot ha^{-1}$, respectively, in 2018; and 7700, 5744 and 5159 $m^3 \cdot ha^{-1}$, respectively, in 2019.

Table 2. Monthly average values of the weather parameters for the irrigation period during the study.

Parameters	April	May	June	July	August	September	October
2018							
T_{max}	22.0	25.6	30.5	33.7	37.7	33.6	26.3
T_{min}	9.5	12.1	15.2	15.9	18.7	18.3	13.1
T_{av}	15.2	18.2	22.5	24.4	27.6	24.9	19.0
RH_{max}	967.3	936.5	93.6	96.1	87.9	89.7	95.3
RH_{min}	44.1	37.3	33.3	27.5	20.7	30.7	41.0
RH_{av}	75.6	71.3	62.4	60.9	51.9	61.9	71.8
Rad	17.3	21.9	24.9	27.0	23.5	19.6	13.9
R	97.2	103.0	5.4	0.0	0.6	21.4	98.4
ET_0	96.6	125.5	150.8	172.1	168.8	125.4	198.1
ETc	57.9	113.0	165.9	206.5	185.6	100.3	49.9
2019							
T_{max}	22.2	30.4	31.3	34.5	36.5	32.4	27.6
T_{min}	7.2	12.2	17.5	17.9	17.9	16.3	11.7
T_{av}	19.8	21.5	22.7	25.8	26.9	23.8	18.9
RH_{max}	97.8	85.2	83.2	84.0	77.2	81.9	90.7
RH_{min}	39.8	23.3	23.4	25.3	18.7	27.6	32.9
RH_{av}	72.2	52.3	51.4	55.4	45.9	54.4	63.2
Rad	1.9	2.1	2.1	2.9	0.8	0.9	0.7
R	71.2	0.0	0.0	0.0	0.0	3.4	10.4
ET_0	111.0	198.0	202.9	238.7	170.1	121.0	76.4
ETc	61.6	126.2	151.3	209.8	140.1	92.8	54.8

R, rainfall (mm); T_{max}, maximum air temperature (°C); T_{min}, minimum air temperature (°C); T_{av}, average air temperature (°C); RH_{max}, maximum relative humidity (%); RH_{min}, minimum relative humidity (%); RH_{av}, average relative humidity (%); Rad, solar radiation ($W \cdot m^{-2}$); R, rainfall (mm); ET_0, reference evapotranspiration (mm); ETc, crop evapotranspiration (mm).

3.2. Physiological Response to Irrigation Treatments

Table 3 displays the physiological response found for Ψ_{leaf}, g_s, and T_C during 2018. The main significant differences among the irrigation treatments were detected for Ψ_{leaf}. In this sense, cv. Marta showed differences at 190, 197, 211, 218, and 225 DOY. For the case of cv. Guara, these differences were detected at 166 and 225 DOY. Finally, regarding cv. Lauranne, significant differences were observed at 190, 197, and 211 DOY. For the remaining variables, only punctual days showed significant differences.

Table 3. Temporal evolution of the physiological variables measured throughout 2018.

DOY	Treat	Marta Ψ_{leaf} (MPa)	Marta g_s (mmol m^{-2} s^{-1})	Marta Tc (°C)	Guara Ψ_{leaf} (MPa)	Guara g_s (mmol m^{-2} s^{-1})	Guara Tc (°C)	Lauranne Ψ_{leaf} (MPa)	Lauranne g_s (mmol m^{-2} s^{-1})	Lauranne Tc (°C)
162	FI	−0.92a	154.50a	21.80a	−0.92a	143.48a	22.68a	−0.97a	129.08a	22.50a
	SDI$_{75}$	−0.82a	153.17a	21.94a	−0.95a	117.80a	23.04a	−0.98a	125.30a	23.51a
	SDI$_{65}$	−0.88a	127.90b	22.39a	−1.04a	174.48a	22.95a	−0.93a	130.25a	23.21a
166	FI	−1.06a	144.27a	27.02a	−0.93a	180.65a	28.29a	−1.05a	187.85a	27.94a
	SDI$_{75}$	−1.13a	160.50a	27.90a	−1.21b	175.07a	28.30a	−1.08a	179.68a	28.18a
	SDI$_{65}$	−1.11a	173.93a	27.53a	−1.22b	191.10a	28.03a	−1.05a	180.88a	28.00a
190	FI	−1.35a	76.28a	31.09a	−1.58a	99.21a	31.49a	−1.54a	112.00a	31.14a
	SDI$_{75}$	−1.44b	84.09a	31.94a	−1.50a	99.83a	32.26a	−1.70b	102.88a	31.97a
	SDI$_{65}$	−1.40ab	79.24a	31.91a	−1.67a	109.66a	32.67a	−1.72b	110.64a	31.99a
197	FI	−1.16a	77.14a	26.96a	−1.44a	79.79a	27.81a	−1.40a	93.25a	28.34a
	SDI$_{75}$	−1.27b	72.86a	27.80a	−1.45a	84.64a	28.45a	−1.50b	89.73a	28.58a
	SDI$_{65}$	−1.31b	78.03a	27.44a	−1.42a	84.13a	28.25a	−1.55b	89.35a	28.68a
206	FI	−1.01a	84.41a	28.93a	−1.38a	107.59a	29.63a	−1.38a	126.57a	27.92b
	SDI$_{75}$	−1.09a	90.90a	29.12a	−1.36a	107.90a	29.68a	−1.21a	128.36a	29.00a
	SDI$_{65}$	−1.06a	89.11a	29.73a	−1.40a	107.34a	29.85a	−1.38a	129.50a	29.12a
211	FI	−1.15a	110.80a	28.39a	−1.49a	120.86a	28.91a	−1.36a	126.43a	28.80a
	SDI$_{75}$	−1.31b	99.64a	28.69a	−1.57a	110.65b	29.04a	−1.42b	133.20a	29.43a
	SDI$_{65}$	−1.38b	96.58a	28.99a	−1.53a	98.80b	29.16a	−1.44b	129.07a	29.21a
218	FI	−1.87a	138.02a	32.85a	−2.17a	154.36a	33.15b	−1.84a	189.04a	33.01a
	SDI$_{75}$	−1.82a	134.86a	33.58a	−2.12a	166.15a	34.28a	−2.05a	181.77a	33.62a
	SDI$_{65}$	−1.68a	140.90a	33.7a	−2.18a	150.73a	34.40a	−1.71a	172.70a	33.66a
225	FI	−1.74a	129.10a	31.83a	−1.76a	138.99a	31.93a	−1.88a	166.89a	30.95b
	SDI$_{75}$	−1.79a	116.47a	32.02a	−2.29b	139.86a	32.78a	−2.10a	165.27a	32.97a
	SDI$_{65}$	−2.03b	122.47a	32.77a	−2.01b	129.44a	32.87a	−1.92a	163.96a	32.92a

Treat, treatment; g_s, stomatal conductance; Ψ_{leaf}, leaf water potential; T_C, canopy temperature; FI, fully irrigated treatment; SDI$_{75}$, sustained deficit irrigation at 75% of the crop irrigation requirements; SDI$_{65}$, sustained deficit irrigation at 65% of the crop irrigation requirements; DOY, day of the year. Different letters represent significant differences ($p < 0.05$) among treatments within each cultivar.

A similar pattern was observed during the second experimental season as shown in Table 4, the Ψ_{leaf} being the physiological parameter that displayed the most perceptible effects in response to the different irrigation treatments.

In this regard, for the case of cv. Marta, these differences during the monitoring period were at 175, 183, 189, 196, 203, 210, and 217 DOY. In the same vein, cv. Guara registered significant differences for Ψ_{leaf} at 162, 175, 183, 189, 196, 203, 210, and 217 DOY. Finally, as was determined for the previous cultivars, cv. Lauranne recorded significant differences throughout the irrigation period for Ψ_{leaf} at 175, 183, 189, 196, 203, and 217 DOY.

Table 4. Temporal evolution of the physiological variables measured throughout 2019.

DOY	Treat	Marta Ψ_{leaf} (MPa)	g_s (mmol m^{-2} s^{-1})	Tc (°C)	Guara Ψ_{leaf} (MPa)	g_s (mmol m^{-2} s^{-1})	Tc (°C)	Lauranne Ψ_{leaf} (MPa)	g_s (mmol m^{-2} s^{-1})	Tc (°C)
	FI	−1.47a	279.70a	29.65a	−1.46a	314.73a	30.24a	−1.41a	271.48a	30.91a
162	SDI75	−1.52a	298.97a	29.94a	−1.75b	280.65a	31.91a	−1.58a	266.93a	30.73a
	SDI65	−1.60a	308.45a	30.54a	−2.11b	274.88a	30.47a	−1.49a	275.62a	30.10a
	FI	−1.42a	274.55a	29.74a	−1.75a	222.67a	29.34b	−1.43a	205.53a	29.25a
175	SDI75	−1.54b	298.87a	28.23a	−2.04b	215.02a	27.02a	−1.87b	206.88a	29.67a
	SDI65	−1.52b	278.13a	29.41a	−1.77a	213.72a	30.06c	−1.83b	192.12a	29.15a
	FI	−1.36a	197.80a	25.95a	−1.61a	199.80a	26.41a	−1.50a	217.97a	25.53a
183	SDI75	−1.52b	190.88a	26.18a	−1.80b	195.37a	26.79a	−1.80b	203.43a	26.01a
	SDI65	−1.54b	192.73a	26.29a	−2.03b	209.57a	26.69a	−1.64b	206.38a	26.31a
	FI	−1.36a	197.80a	25.95b	−1.61a	199.80a	26.41a	−1.50a	217.97a	25.53a
189	SDI75	−1.52b	190.88a	26.18a	−1.80b	195.37a	26.79a	−1.80b	203.43a	26.01a
	SDI65	−1.54b	192.73a	26.29a	−2.03b	209.57a	26.69a	−1.64b	206.38a	26.31ab
	FI	−1.08a	175.82a	28.83a	−1.4a	165.17a	29.26a	−1.31a	163.80a	29.10a
196	SDI75	−1.29b	173.17a	29.25a	−1.74b	174.03a	29.96a	−1.57b	164.20a	29.06a
	SDI65	−1.28b	172.30a	28.95a	−1.71b	175.37a	30.00a	−1.53b	158.13a	29.15a
	FI	−1.67a	152.37a	31.83a	−1.88a	163.55a	30.79b	−1.69a	161.07a	31.26a
203	SDI75	−1.69a	144.55a	31.69a	−2.01b	145.10a	31.63a	−1.90b	157.03a	30.95a
	SDI65	−1.87b	155.22a	31.79a	−2.11b	155.72a	31.83a	−1.89b	170.28a	31.16a
	FI	−1.19a	165.10a	27.53a	−1.38a	177.73a	26.78a	−1.44a	174.07a	27.45a
210	SDI75	−1.26a	168.58a	27.51a	−1.55b	187.20a	26.97a	−1.57a	185.95a	27.85a
	SDI65	−1.35b	177.20a	27.65a	−1.50b	182.55a	27.67a	−1.49a	188.20a	27.89a
	FI	−1.55a	180.50a	29.44a	−1.73a	179.65a	29.20a	−1.72a	191.52a	29.73a
217	SDI75	−1.80b	167.98a	29.47a	−1.95b	194.50a	29.65a	−1.97b	184.35a	29.81a
	SDI65	−1.72b	176.20a	29.41a	−1.90b	195.53a	29.49a	−1.95b	185.43a	29.45a

Treat, treatment; g_s, stomatal conductance; Ψ_{leaf}, leaf water potential; T_C, canopy temperature; FI, fully irrigated treatment; SDI75, sustained deficit irrigation at 75% of the crop irrigation requirements; SDI65, sustained deficit irrigation at 65% of the crop irrigation requirements; DOY, day of the year. Different letters represent significant differences ($p < 0.05$) among treatments within each cultivar.

3.3. Water-Stress Baselines for Each Cultivar and Irrigation Treatment, and Their Interactions

Taking as reference the T_{air} values registered during the data acquisition (Figure 2), the $\Delta T_{canopy-air}$ was calculated, and afterwards, the relationships with measured VPD were defined for each treatment and cultivar, considering the whole dataset obtained in both experimental seasons (Figure 3, Table 5).
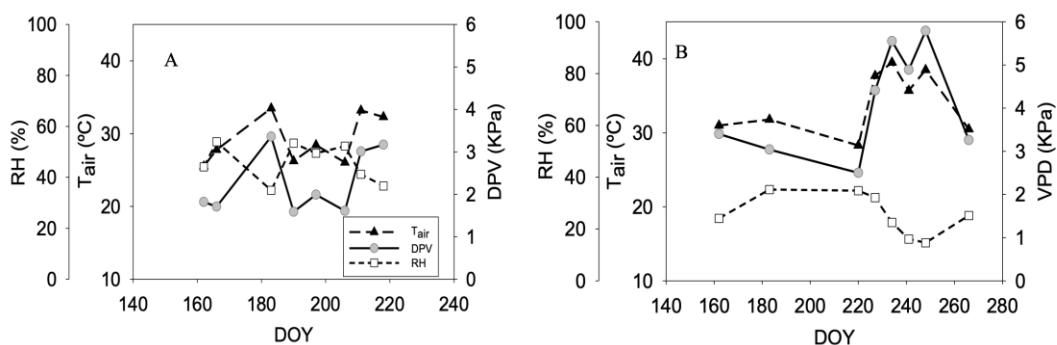

Figure 2. Meteorological conditions during the data collection in 2018 (**A**) and 2019 (**B**). T_{air}, air temperature; RH, relative humidity; VPD, vapor pressure deficit; DOY, day of the year.
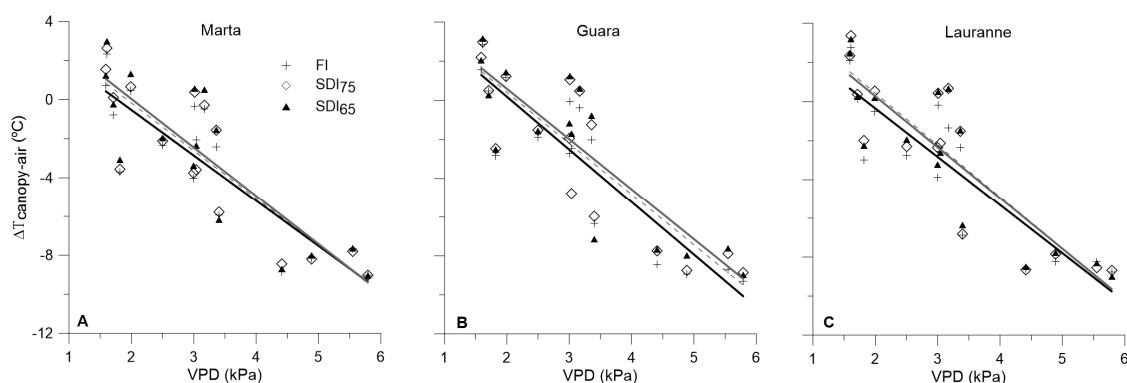
Figure 3. Water-stress baselines for cvs. Marta (**A**), Guara (**B**), and Lauranne (**C**). Black continuous, discontinuous and grey lines are the regressions functions that represent the non-water-stress baseline for fully irrigated (FI), and the water-stress baselines for sustained deficit irrigation at 75% of the crop irrigation requirements (SDI$_{75}$) and sustained deficit irrigation at 65% of the crop irrigation requirements (SDI$_{65}$), respectively.

Table 5. Fitted parameters for the non-water-stress baselines and water-stress baselines for the almond cultivars and irrigation treatments.

Baseline	cv. Guara			cv. Marta			cv. Lauranne		
	Slope	Intercept	R^2	Slope	Intercept	R^2	Slope	Intercept	R^2
NWSB	−2.71a	5.60a	0.82	−2.33a	4.14a	0.75	−2.48a	4.62a	0.78
WSB$_{75}$	−2.62a	5.65a	0.76	−2.45a	4.73a	0.75	−2.66a	5.75a	0.77
WSB$_{65}$	−2.58a	5.76a	0.74	−2.49a	5.01a	0.74	−2.62a	5.51a	0.77

NWSB, non-water-stress baseline defined according to the registered values in full irrigated treatment; WSB$_{75}$, water-stress baseline according to the registered values in the sustained deficit irrigation at 75% of the crop irrigation requirements; WSB$_{65}$, water-stress baseline according to the registered values in the sustained deficit irrigation at 65% of the crop irrigation requirements. Equal letters within each column are not significantly different ($p < 0.05$).

As shown in Table 5, within each cultivar, the ANCOVA did not manifest differences in terms of the slope and the interception point for any of the studied cultivars. This absence of differences is in accordance with the previous results noted in relation to T_C and g_s, parameters without differences during the monitoring period. Moreover, this difference could be associated with the inherent variability of the experiment, especially, in T_C readings. In this agreement, within each treatment it was observed Tc variations of ±0.5, ±0.9, and ±1.5 °C in the FI, SDI$_{75}$, and SDI$_{65}$, respectively. This variability was also higher the more remarkable the imposed water stress was. Moreover, a higher variability was found in cv. Guara while cvs. Marta and Lauranne showed lower and similar variability trends.

Considering this absence of differences between the irrigation treatments, there was defined a single WSB for each cultivar with the whole dataset (Table 6). These reference water-stress baselines (rWSB) would allow knowing an optimum $\Delta T_{canopy-air}$, establishing the lower and upper limits from the NWSB and WSB previously defined for the FI and SDI treatments (Figure 4).

Table 6. Fitted parameters for the reference water-stress baselines (rWSB) for each cultivar.

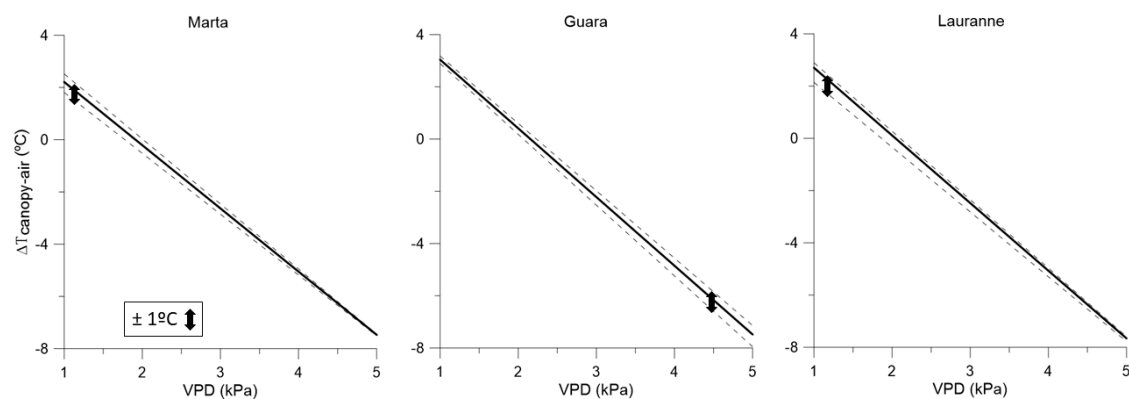| Cultivars	Slope	Intercept	R^2
Marta	−2.42	4.63	0.74
Guara	−2.63	5.67	0.77
Lauranne	−2.59	5.29	0.74

Figure 4. Reference water-stress baselines (rWSB, continuous lines) for cvs. Marta (**A**), Guara (**B**) and Lauranne (**C**). The upper and lower discontinuous lines correspond to the water stress and non-water stress baselines functions defined under sustained deficit irrigation at 65% of the irrigation requirements and fully irrigated conditions, respectively. Black arrows indicate the maximum increment of canopy temperature, with the aim of establishing the threshold limits for irrigation scheduling in the studied almond cultivars.

According to our findings, the maximum IT_C reported for each cultivar was ~1.0 °C (Figure 4); that is, the highest differences between the FI and SDI_{65} strategies would report increases beyond the lower limit around a degree in the sunny side of the almond canopy. Moreover, this deviation would be different depending on the cultivar. For the case of cvs. Marta and Lauranne, the maximum IT_C were detected in the lower ranges of the VPD that contrasts with cv. Guara.

Finally, taking into consideration the NWSB and WSB for each treatment and cultivar, and with the aim of establishing a useful threshold limit that ensures the maximum water savings, the CWSI on a monthly basis was estimated (Figure 5). It is noticeable the progressive increase along the kernel-filling period, especially in cvs. Marta and Lauranne, displaying a progressive rise because of the water-stress accumulation. Moreover, in cv. Guara and cv. Marta, the SDI_{65} reported a CWSI higher than those obtained in cv. Lauranne, where in the latter the SDI_{75} registered similar values of the CWSI. For cv. Guara, the maximum CWSI was reached under SDI_{65}, with values close to 0.14. Similar results were found for cv. Lauranne (~0.15), whereas in cv. Marta these values were somewhat lower, roughly 0.12.
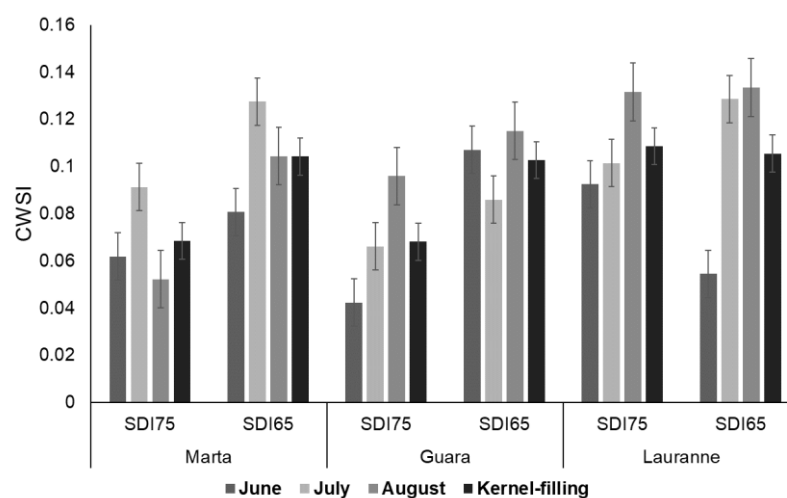

Figure 5. The crop water-stress index (CWSI) on a monthly basis for the water-stressed treatments (SDI) and studied cultivars. SDI_{75}, irrigated at 75% of the irrigation requirements; SDI_{65}, irrigated at 65% of the irrigation requirements. Vertical bars are standard deviation.

3.4. Linking the Yield with Water-Stress Baselines Defined for Each Cultivar and Irrigation Treatment

After estimating the different WSBs, the final yield was analyzed for each irrigation treatment and cultivar (Figure 6). This fact is necessary to define the threshold values of $\Delta T_{canopy-air}$ and CWSI to minimize the yield losses and maximize the water savings (in case of obtaining significant differences between irrigation treatments). On average, for cvs. Marta and Lauranne, no differences were observed, evidencing that water withholding close to 35% of the irrigation requirements would not promote yield losses, at least during two consecutive seasons. Something different was determined for cv. Guara. In this case, in spite of not finding significant differences, there was a trend between the yield loss and water stress imposed; that is, the obtained values for SDI_{75} and SDI_{65} were notably lower than those observed under FI, with yield reductions of 11% and 15%; respectively.
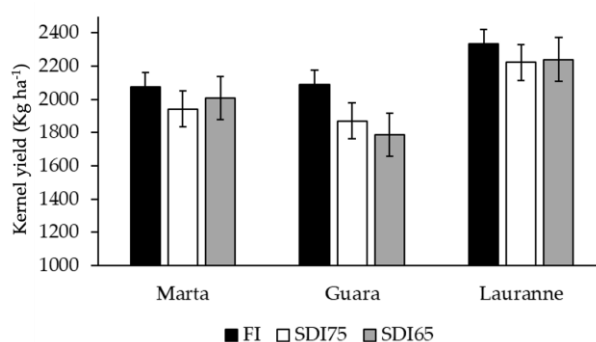
Figure 6. Average kernel yield for the studied almond cultivars during the study. FI, fully irrigated at 100% of irrigation requirements; SDI_{75}, irrigated at 75% of the irrigation requirements; SDI_{65}, irrigated at 65% of the irrigation requirements. Vertical bars are standard deviation.

4. Discussion

The focus of this paper was to assess the use of thermal data as indicator of crop water status instead of discontinuous measurements, such as Ψ_{leaf} or g_s, which are highly time-consuming with a huge number of measurements that are needed for taking decisions.

Considering the results showed in this work, the Ψ_{leaf} was the parameter that showed the highest differences between treatments in the two-year experiment, relative to g_s and T_C (Tables 3 and 4). It is remarkable that the decreasing pattern in Ψ_{leaf} was not followed by g_s, likely because of the lower capacity of almond trees to regulate their stomata under mild water-stress situations [3,34]. These findings were in agreement with other works [35,36], showing that under mild stress, almond decreases Ψ_{leaf} significantly more than g_s, which remains fairly constant until severe water stress. As g_s tightly controls plant transpiration, this, in turn, determines to a great extent the leaf temperature. The lack of significant differences in g_s among the irrigation treatments and for none of the cultivars support why there were also no differences between T_C and WSBL. In addition, plant transpiration, in which g_s determines photosynthesis, in conjunction with turgor, is liable for growth and yield. Accordingly, fruit yield did not show relevant differences among the irrigation treatments for cvs. Marta and Lauranne, although these were more evident for cv. Guara. In accordance with our data and to previous works, it seems that to detect a higher response of g_s to water stress it would be necessary to impose more severe water-stress conditions; then the stomatal response would be mainly governed by the crop water status [10,22].

The use of thermal data as indicator of crop water status has been implemented in different works to solve the drawback that Ψ_{leaf} or g_s carried out with their development [27,36]. In order to define the most proper strategy, many authors have discussed the best time to capture the images, the tree area or the time range to take the images. In this sense, González-Dugo et al. [37] concluded that, for the case of citrus trees, the best moment to capture the thermal images would be between 11:20 and 12:00. They also observed that the maximum differences between the control and stressed trees ranged between 1.5

and 2.5 °C. Their results agree with those obtained in this experiment, in which the maximum difference between the FI and SDI treatments is ±1 °C (Figure 4). In the same line, García-Tejero et al. [33] in an experiment with almond (cv. Guara) concluded that the best moment to capture thermal images was between 11:30 and 14:00 in the sunny exposed side of the tree, when the maximum differences of T_C between the FI and DI treatments were reached. Therefore, these differences were always from 0.5 to 1.5 °C when a water restriction close to 50% of the irrigation requirements was imposed, similar to findings that was obtained in the present work.

Despite Tc not always having a direct relationship with Ψ_{leaf} or g_s, due to the large environmental variability, the use of different thermal indexes that normalize this parameter to the meteorological conditions make this tool suitable to determine the crop water status [24]. In this study the use of the index $\Delta T_{canopy-air}$ allowed to establish the NWSB and WSB for three almond cultivars, adjusting these values with those of the VPD registered. In this context, Bellvert et al. [38] outlined that different WSB can be obtained, and their main differences could be associated with their intercept point; these differences being associated to variation in the crop water status [19,20] or the crop phenological stage. Similarly, García-Tejero et al. [28], for mature almond trees, reported differences in the interception point between different WSBs within a cultivar subjected to different irrigation doses. These results agree with that found in this work (Figure 3, Table 5). In this line, although the ANCOVA did not evidence significant differences in the slope and interception point among the irrigation doses imposed in each cultivar, we observed maximum differences between the NWSB and WSB close to 1.0 °C, comparable to findings by García-Tejero et al. [28] or García-Tejero et al. [33]. The main differences among these results and those reported by the authors would be mainly in the slope of the functions calculated for the studied cultivars. Thus, González-Dugo et al. [37] or García-Tejero et al. [28] reported similar slopes for mature almond trees, cv. Guara, which were growing under similar climatic conditions. In our case, the obtained slopes were substantially different; this being an important fact to be considered in future works. Thus, this fact could be due to the tree age and this work being defined in young trees, whereas the previous works were developed in mature almond trees, in which the transpiration capacity could have substantially changed.

Authors such as Romero-Trigueros et al. [39] largely discussed the advantages of this type of functions when these are applied in isohydric crops, with a higher capacity of stomatal regulation when they are subjected to water withholding. This is not the case for almond, with a downregulation of stomatal conductance, resulting in similar T_C values for trees subjected to different irrigation doses. Considering that no differences were found among the irrigation treatments, the rWSB defined for each cultivar would be a suitable option for irrigation scheduling under moderate scenarios of water scarcity, knowing that there were no differences in productive terms with water around 2000 m^3 × ha^{-1} (Figure 6).

Finally, in spite of to the absence of significant differences in yield for the three studied cultivars, cv. Guara was affected with a progressive depletion in relation to the water stress imposed. Confronting these results with the maximum IT_C registered, cv. Guara was the unique in which IT_C increased for major values of VPD, and it could demonstrate a higher sensitivity to the SDI strategy than the remaining cultivars, especially when atmospheric demand is higher. Likewise, the absence of differences in terms of yield has been widely stated by several authors [10,40–42] and, therefore, this reaction ratifies the advantages of this agronomic practices for almond cultivation in arid and semi-arid environments.

5. Conclusions

From the research that has been performed in this paper, it is possible to conclude that the $\Delta T_{canopy-air}$ and its related thermal indexes (CWSI and IT_C) are precise indicators of the crop water status in young almond trees. In detail, the use of $\Delta T_{canopy-air}$ to establish the NWSB and WSBs for different cultivars and water-stress levels would offer an optimum tool for irrigation management differentiated by cultivar and water restrictions. On the other hand, considering the three cultivars

studied, cv. Guara offered a higher sensitivity to water stress, as in yield reductions in terms of its physiological response. Following the proposed methodology of this study, using thermal data, it would be possible to materialize other WSB for different cultivars and tree ages for alternative irrigation programming, especially when DI is used. However, taking into consideration that there were no differences found in yield between the water-stressed and non-stressed treatments, future essays imposing more severe water stress should be considered, in order to ensure obtaining the maximum threshold value (in terms of the CWSI or ITc) that would not significantly impact yield, explicitly under long-term irrigation periods.

References

1. Iglesias, A.; Mougou, R.; Moneo, M.; Quiroga, S. Towards adaptation of agriculture to climate change in the Mediterranean. *Reg. Environ. Chang.* **2011**, *11*, 159–166. [CrossRef]

2. Fereres, E.; Soriano, M.A. Deficit irrigation for reducing agricultural water use. *J. Exp. Bot.* **2007**, *58*, 147–159. [CrossRef] [PubMed]

3. Fernández, J.E. Understanding olive adaptation to abiotic stresses as a tool to increase crop performance. *Environ. Exp. Bot.* **2014**, *103*, 158–179. [CrossRef]

4. Durán Zuazo, V.H.; Rodríguez Pleguezuelo, C.R.; Franco Tarifa, D. Impact of sustained-deficit irrigation on tree growth, mineral nutrition, fruit yield and quality of mango in Spain. *Fruits* **2011**, *66*, 257–268. [CrossRef]

5. Buchner, R.P.; Fulton, A.E.; Gilles, C.K.; Prichard, T.L.; Lampinen, B.D.; Shackel, K.A.; Metcalf, S.G.; Little, C.C.; Schwankl, L.J. Effects of regulated deficit irrigation on walnut grafted on "Northern California Black" or "Paradox" rootstock. *Acta Hortic.* **2008**, *792*, 141–146. [CrossRef]

6. García-Tejero, I.; Romero-Vicente, R.; Jiménez-Bocanegra, J.A.; Martínez-García, G.; Durán Zuazo, V.H.; Muriel-Fernández, J.L. Response of citrus trees to deficit irrigation during different phenological periods in relation to yield, fruit quality, and water productivity. *Agric. Water Manag.* **2010**, *97*, 689–699. [CrossRef]

7. Memmi, H.; Gijón, M.C.; Couceiro, J.F.; Pérez-López, D. Water stress thresholds for regulated deficit irrigation in pistachio trees: Rootstock influence and effects on yield quality. *Agric. Water Manag.* **2016**, *164*, 58–72. [CrossRef]

8. Caracterización del sector de la almendra en Andalucía. Secretaría General de Agricultura y Alimentación. Junta de Andalucía. 2016, 34. Available online: https://www.juntadeandalucia.es/export/drupaljda/estudios_informes/16/12/Caracterizaci%C3%B3n%20del%20sector%20de%20la%20almendra_0.pdf (accessed on 5 April 2020).

9. Egea, G.; González-Real, M.M.; Baille, A.; Nortes, P.A.; Sánchez-Bel, P.; Domingo, R. The effects of contrasted deficit irrigation strategies on the fruit growth and kernel quality of mature almond trees. *Irrig. Sci.* **2009**, *36*, 1–8. [CrossRef]

10. Romero, P.; Botia, P.; Garcia, F. Effects of regulated deficit irrigation under subsurface drip irrigation conditions on vegetative development and yield of mature almond trees. *Plant Soil* **2004**, *260*, 169–181. [CrossRef]

11. Espadafor, M.; Orgaz, F.; Testi, L.; Lorite, I.J.; González-Dugo, V.; Fereres, E. Responses of transpiration and transpiration efficiency of almond trees to moderate water deficits. *Sci. Hortic. (Amsterdam)* **2017**, *225*, 6–14. [CrossRef]

12. Nortes, P.A.; Gonzalez-Real, M.M.; Egea, G.; Baille, A. Seasonal effects of deficit irrigation on leaf photosynthetic traits of fruiting and non-fruiting shoots in almond trees. *Tree Physiol.* **2009**, *29*, 375–388. [CrossRef] [PubMed]

13. Girona, J.; Mata, M.; Marsal, J. Regulated deficit irrigation during the kernel-filling period and optimal irrigation rates in almond. *Agric. Water Manag.* **2005**, *75*, 152–167. [CrossRef]

14. Rojo, F.; Kizer, E.; Upadhyaya, S.; Ozmen, S.; Ko-Madden, C.; Zhang, Q. A Leaf Monitoring System for Continuous Measurement of Plant Water Status to Assist in Precision Irrigation in Grape and Almond crops. *IFAC-PapersOnLine* **2016**, *49*, 209–215. [CrossRef]

15. Dhillon, R.; Rojo, F.; Roach, J.; Upadhyaya, S.; Delwiche, M. A Continuous Leaf Monitoring System for Precision Irrigation Management in Orchard Crops. *Tarım Makinaları Bilim. Derg.* **2014**, *10*, 267–272.

16. Fernández, J.E. Plant-based methods for irrigation scheduling of woody crops. *Horticulturae* **2017**, *3*, 35. [CrossRef]

17. Jackson, R.D.; Idso, S.B.; Reginato, R.J.; Pinter, P.J. Canopy temperature as a crop water stress indicator. *Water Resour. Res.* **1981**, *17*, 1133–1138. [CrossRef]

18. Idso, S.B. Non-water-stressed baselines: A key to measuring and interpreting plant water stress. *Agric. Meteorol.* **1982**, *27*, 59–70. [CrossRef]

19. Jones, H.G. Irrigation scheduling: Advantages and pitfalls of plant-based methods. *J. Exp. Bot.* **2004**, *55*, 2427–2436. [CrossRef]

20. Jiménez-Bello, M.A.; Ballester, C.; Castel, J.R.; Intrigliolo, D.S. Development and validation of an automatic thermal imaging process for assessing plant water status. *Agric. Water Manag.* **2011**, *98*, 1497–1504. [CrossRef]

21. Egea, G.; Padilla-Díaz, C.M.; Martinez-Guanter, J.; Fernández, J.E.; Pérez-Ruiz, M. Assessing a crop water stress index derived from aerial thermal imaging and infrared thermometry in super-high density olive orchards. *Agric. Water Manag.* **2017**, *187*, 210–221. [CrossRef]

22. García-Tejero, I.; Gutiérrez Gordillo, S.; Souza, L.; Cuadros-Tavira, S.; Durán Zuazo, V.H. Fostering sustainable water use in almond (*Prunus dulcis* Mill.) orchards in a semiarid Mediterranean environment. *Arch. Agron. Soil Sci.* **2019**, *65*, 164–181. [CrossRef]

23. Pou, A.; Diago, M.P.; Medrano, H.; Baluja, J.; Tardaguila, J. Validation of thermal indices for water status identification in grapevine. *Agric. Water Manag.* **2014**, *134*, 60–72. [CrossRef]

24. Poirier-Pocovi, M.; Volder, A.; Bailey, B.N. Modeling of reference temperatures for calculating crop water stress indices from infrared thermography. *Agric. Water Manag.* **2020**, *233*, 106070. [CrossRef]

25. Jones, H.G.; Serraj, R.; Loveys, B.R.; Xiong, L.; Wheaton, A.; Price, A.H. Thermal infrared imaging of crop canopies for the remote diagnosis and quantification of plant responses to water stress in the field. *Funct. Plant Biol.* **2009**, *36*, 978–989. [CrossRef]

26. Jones, H.G.; Vaughan, R. Remote Sensing of Vegetation: Principles, Techniques and Applications. *Soil Use Manag.* **2012**, *28*, 134. [CrossRef]

27. García-Tejero, I.F.; Hernández, A.; Padilla-Díaz, C.M.; Diaz-Espejo, A.; Fernández, J.E. Assessing plant water status in a hedgerow olive orchard from thermography at plant level. *Agric. Water Manag.* **2017**, *188*, 50–60. [CrossRef]

28. García-Tejero, I.F.; Gutiérrez-Gordillo, S.; Ortega-Arévalo, C.; Iglesias-Contreras, M.; Moreno, J.M.; Souza-Ferreira, L.; Durán Zuazo, V.H. Thermal imaging to monitor the crop-water status in almonds by using the non-water stress baselines. *Sci. Hortic.* **2018**, *238*, 91–97. [CrossRef]

29. Idso, S.B.; Jackson, R.D.; Pinter, P.J.; Reginato, R.J.; Hatfield, J.L. Normalizing the stress-degree-day parameter for environmental variability. *Agric. Meteorol.* **1981**, *24*, 45–55. [CrossRef]

30. Peel, M.C.; Finlayson, B.L.; McMahon, T.A. Updated world map of the Köppen-Geiger climate classification. *Hydrol. Earth Syst. Sci.* **2007**, *11*, 1633–1644. [CrossRef]

31. Allen, R.G.; Pereira, L.S.; Raes, D.; Smith, M. *Crop Evapotranspiration—Guidelines for Computing Crop Water Requirements-Irrigation and Drainage Paper 56*; Food and Agriculture Organization (FAO): Rome, Italy, 1998; Available online: http://www.fao.org/docrep/x0490e/x0490e00.htm (accessed on 12 February 2020).

32. García-Tejero, I.F.; Hernandez, A.; Rodriguez, V.M.; Ponce, J.R.; Ramos, V.; Muriel, J.L.; Durán Zuazo, V.H. Estimating Almond Crop Coefficients and Physiological Response to Water Stress in Semiarid Environments (SW Spain). *J. Agric. Sci. Technol.* **2015**, *17*, 1255–1266.

33. García-Tejero, I.F.; Rubio, A.E.; Viñuela, I.; Hernández, A.; Gutiérrez-Gordillo, S.; Rodríguez-Pleguezuelo, C.R.; Durán Zuazo, V.H. Thermal imaging at plant level to assess the crop-water status in almond trees (cv. Guara) under deficit irrigation strategies. *Agric. Water Manag.* **2018**, *208*. [CrossRef]

34. Fu, X.; Meinzer, F.C. Metrics and proxies for stringency of regulation of plant water status (iso/anisohydry): A global data set reveals coordination and trade-offs among water transport traits. *Tree Physiol.* **2018**, *39*, 122–134. [CrossRef] [PubMed]

35. Hernandez-Santana, V.; Rodriguez-Dominguez, C.M.; Fernández, J.E.; Diaz-Espejo, A. Role of leaf hydraulic conductance in the regulation of stomatal conductance in almond and olive in response to water stress. *Tree Physiol.* **2016**, *36*, 725–735. [CrossRef] [PubMed]

36. Rodriguez-Dominguez, C.M.; Buckley, T.N.; Egea, G.; de Cires, A.; Hernandez-Santana, V.; Martorell, S.; Diaz-Espejo, A. Most stomatal closure in woody species under moderate drought can be explained by stomatal responses to leaf turgor. *Plant Cell Environ.* **2016**, *39*, 2014–2026. [CrossRef]

37. González-Dugo, V.; Zarco-Tejada, P.J.; Fereres, E. Applicability and limitations of using the crop water stress index as an indicator of water deficits in citrus orchards. *Agric. For. Meteorol.* **2014**, *198–199*, 94–104. [CrossRef]

38. Bellvert, J.; Zarco-Tejada, P.J.; Girona, J.; Fereres, E. Mapping crop water stress index in a 'Pinot-noir' vineyard: Comparing ground measurements with thermal remote sensing imagery from an unmanned aerial vehicle. *Precis. Agric.* **2014**, *15*, 361–376. [CrossRef]

39. Romero-Trigueros, C.; Bayona Gambín, J.M.; Nortes Tortosa, P.A.; Alarcón Cabañero, J.J.; Nicolás, E.N. Determination of Crop Water Stress index by infrared thermometry in grapefruit trees irrigated with saline reclaimed water combined with deficit irrigation. *Remote Sens.* **2019**, *11*, 757. [CrossRef]

40. Egea, G.; Nortes, P.A.; Domingo, R.; Baille, A.; Pérez-Pastor, A.; González-Real, M.M. Almond agronomic response to long-term deficit irrigation applied since orchard establishment. *Irrig. Sci.* **2013**, *31*, 445–454. [CrossRef]

41. López-López, M.; Espadador, M.; Testi, L.; Lorite, I.J.; Orgaz, F.; Fereres, E. Water use of irrigated almond trees when subjected to water deficits. *Agric. Water Manag.* **2018**, *195*, 84–93. [CrossRef]

42. Monks, D.P.; Taylor, C.; Sommer, K.; Treeby, M.T. Deficit irrigation of almond trees did not decrease yield. *Acta Hortic.* **2017**, *1150*, 251–260. [CrossRef]